RSC Advances

PAPER

View Article Online
View Journal | View Issue

Cite this: *RSC Adv.*, 2020, **10**, 14451

Inorganic/organic nanocomposite ion gels with well dispersed secondary silica nanoparticles†

Tomoki Yasui, Eiji Kamio * and Hideto Matsuyama *

Received 17th March 2020
Accepted 27th March 2020

DOI: 10.1039/d0ra02478c

rsc.li/rsc-advances

We have previously reported tough inorganic/organic nanocomposite (NC) ion gels composed of silica particles and poly(*N*,*N*-dimethylacrylamide) (PDMAAm) networks and a large amount of ionic liquid. In this study, the network structure and toughening mechanism of NC ion gels were investigated. The NC ion gels showed characteristic mechanical properties; *i.e.* the stress was significantly increased at a highly elongated state. In addition, the NC ion gels showed an almost elastic mechanical property, which was completely different from that of our other developed inorganic/organic tough ion gels named double-network (DN) ion gels. It was found from structural observation that secondary silica nanoparticles dispersed well in the NC ion gel. It was also found that some of the secondary silica nanoparticles had a ring-like structure which would incorporate PDMAAm chains. From the silica particle content dependency on stress–strain curves of inorganic/organic NC ion gels, it was inferred that the secondary silica particles could serve as a movable cross-linker of PDMAAm chains in the NC ion gel.

Introduction

Ion gels are gels containing ionic liquids (ILs) that exhibit gel-based quasi-solid properties in addition to IL-based properties, such as nonvolatility, nonflammability, high ionic conductivity, high CO_2 solubility, and high thermal, chemical, and electrochemical stabilities. Ion gels are expected to be applied in electrochemical devices, actuators, and gas separation membranes.[1–14] However, the practical applications of ion gels are limited because of their low mechanical strength. Therefore, the development of tough ion gels has attracted increasing interest.

Several types of tough ion gels have been prepared using different concepts, such as tetra-polyethylene glycol (PEG) network-based ion gels,[15] triblock copolymer-based ion gels,[16] and organic/organic double network (DN)-based ion gels.[13,17–20] These tough ion gels showed not only excellent mechanical strength but also the unique IL properties.

Recently, we reported two types of ion gels prepared *via* one-pot/two-step network formation of inorganic/organic network, which were composed of inorganic silica particle aggregates and poly(*N*,*N*-dimethylacrylamide) (PDMAAm) organic networks.[21] When the inorganic aggregates were formed before the organic network formation, the DN ion gels having interpenetrating inorganic/organic network were formed. Meanwhile, inorganic/organic nanocomposite (NC) ion gels were formed when the inorganic aggregates formed after the organic network formation. The mechanical properties of these ion gels differed vastly from each other, even though both gels indicated superior mechanical strength compared with a PDMAAm single-network (SN) ion gel. The inorganic/organic DN ion gels showed clear mechanical hysteresis, while the inorganic/organic NC ion gels showed an elastic behavior. Despite the unique mechanical behaviors, such as excellent mechanical strength and elastic behavior, the network structure and toughening mechanism of the inorganic/organic NC ion gel remained unknown.

The inorganic/organic NC ion gels showed specific stress–strain curves of which stress significantly increased when the gel was highly elongated.[21] These specific mechanical behaviors are similar to those of slide ring (SR) hydrogels reported by Ito *et al.*[22–27] The SR gels are composed of a polyrotaxane network, which is composed of poly(ethylene oxide) as an axis polymer and α-cyclodextrin as ring molecules. In the SR gels, the ring molecules can serve as a movable cross-linker for the axis polymer when the ring molecules are chemically cross-linked. Owing to the movable cross-link function by ring molecules, the SR gels showed specific J-shaped stress–strain curves and a nonhysteresis loop.[27] We speculated that the characteristic mechanical properties and the toughening mechanism of the inorganic/organic NC ion gels were attributed to the movable cross-linker because the stress–strain behavior of the inorganic/organic NC ion gels was similar to that of the SR gels. If the movable cross-link phenomenon occurred in the inorganic/

Research Center for Membrane and Film Technology, Department of Chemical Science and Engineering, Kobe University, 1-1 Rokkodai-cho, Nada-ku, Kobe, Hyogo 657-8501, Japan. E-mail: matuyama@kobe-u.ac.jp; e-kamio@people.kobe-u.ac.jp

† Electronic supplementary information (ESI) available: Differential stress–strain curve of inorganic/organic NC ion gel and PDMAAm SN ion gel, TEM image of inorganic/organic DN ion gel, photographs of inorganic/organic NC, DN, and PDMAAm SN ion gel, and toughening mechanism of inorganic/organic NC ion gel. See DOI: 10.1039/d0ra02478c

organic NC ion gels, silica particles in the ion gels should behave as the ring by incorporating PDMAAm chains in the particles to serve as a movable cross-linker for the PDMAAm network.

To demonstrate the hypothesis above, in this study, the network structure and mechanical properties of the inorganic/organic NC gel were investigated. The mechanical properties of the inorganic/organic NC ion gels with various silica particle contents were measured using a uniaxial stretch test and compared with that of SR hydrogel. The structure of the silica particles and their dispersion state in the inorganic/organic NC ion gels were observed using transmission electron microscopy (TEM) to confirm the structure of the silica nanoparticles formed in the NC ion gels. Based on the results of mechanical properties and TEM observation, the hypothesis on the toughening mechanism of the inorganic/organic NC ion gel is discussed.

Experimental section

Materials

As an IL, 1-butyl-3-methylimidazolium bis(trifluoromethylsulfonyl)imide ([C_4mim][Tf_2N]) (Sigma-Aldrich Co., St. Louis, MO, U.S.A.) was used after eliminating the dissolved water by bubbling dry nitrogen through the IL for more than 15 min. *N*,*N*-dimethylacrylamide (DMAAm, Tokyo Chemical Industry Co., Tokyo, Japan) as a monomer of PDMAAm, 2-oxoglutaric acid (OA, Tokyo Chemical Industry Co.) as a photo radical initiator, and *N*,*N*′-methylenebis(acrylamide) (MBAA, FUJIFILM Wako Pure Chemicals Corporation, Osaka, Japan) as a chemical cross-linker of PDMAAm were used to form an organic PDMAAm network in the IL. DMAAm and OA were used as received. MBAA was used after purification by recrystallization in ethanol. Tetraethyl orthosilicate (TEOS, Sigma-Aldrich Co.) was used to form the silica particle without further purification. Formic acid (FUJIFILM Wako Pure Chemicals Corporation) was used as a solvolytic agent for the sol–gel reaction of TEOS without further purification.

Preparation of inorganic/organic NC ion gels and PDMAAm SN ion gel

Inorganic/organic NC ion gels were prepared *via* a one-pot/two-step process, inducing a photic-initiated free-radical polymerization of DMAAm first, followed by a thermally initiated sol–gel reaction of TEOS in the IL.[21] For example, a precursor solution was prepared by mixing 7.92 g of [C_4mim][Tf_2N], 1.10 g of TEOS, 1.57 g of DMAAm (molar ratio of TEOS/DMAAm = 1/3 mol mol^{-1}), 9.8 mg of MBAA (0.4% of DMAAm in mole), and 2.3 mg of OA (0.1% of DMAAm in mole) until the solution became completely transparent. Subsequently, 1.90 g of formic acid was gently added to the precursor solution and stirred until it was completely dissolved. The solution was injected into a mold comprising two glass plates with a fluorinated ethylene propylene copolymer film and a poly(tetrafluoroethylene) spacer (1.0 mm thickness) and then irradiated by a 365 nm ultraviolet light in an incubator at 293 K for 9 h to form a PDMAAm network. Subsequently, the ion gel was placed in a thermostat oven at 323 K for 48 h for silica particle formation. The obtained ion gel was maintained at 373 K for 12 h under vacuum to remove the formic acid, unreacted monomer, and generated ethanol through the sol–gel reaction of TEOS. To evaluate the effect of silica particle content on the mechanical property of the inorganic/organic NC ion gels, the silica particle content was controlled from 1.1 wt% to 5.5 wt%. The content of PDMAAm in the inorganic/organic NC ion gel was fixed at 17 wt% for every sample by controlling the [C_4mim][Tf_2N] content.

For comparison, the inorganic/organic DN ion gels were prepared by swapping the formation order of the PDMAAm network and silica particle from the same precursor solution of the inorganic/organic NC ion gels, *i.e.* the thermally initiated sol–gel reaction of TEOS was performed first, followed by the photic-initiated free-radical polymerization of DMAAm. Additionally, a PDMAAm SN ion gel was prepared in the same method without using the chemicals for the sol–gel reaction of TEOS. In the DN and SN gels, the content of PDMAAm was fixed at 17 wt%, which was the same as that of NC gel, by controlling the content of [C_4mim][Tf_2N].

Mechanical property measurement

A uniaxial stretch test of inorganic/organic NC ion gels was performed using an automatic recording universal testing instrument (EZ-LX, Shimadzu Co., Kyoto, Japan) at 298 K. A dumbbell-shaped specimen (length, width, thickness: 75.0, 4.0, 1.0 mm) was used for the uniaxial stretching test. Because the inorganic/organic NC ion gels contained no volatile components, the mechanical properties could be measured in an open environment without considering any composition change during the measurement. For all measurements, the sample was attached to the instrument at a distance of 35 mm between the jigs. A uniaxial stretching test was conducted by stretching the sample at a constant strain rate of 100 mm min^{-1}. In the cyclic loading–unloading test, stretching and return operations were performed to increase the maximum strain in steps of 0.5 until the sample broke.

TEM observation

The silica particle in the inorganic/organic NC ion gels was observed using field-emission transmission electron microscopy (FE-TEM) (JEM-2100F, JEOL Ltd., Tokyo, Japan). The IL in the inorganic/organic NC ion gels was replaced with epoxy resin to prepare ultrathin sections. A 1 mm cubic sample of the ion gel was immersed in a sufficient volume of ethanol for 12 h to swap the IL in the ion gels for ethanol. The sample was immersed in a solution of epoxy resin (Plain Resin Kit, Nisshin EM Co., Ltd., Tokyo, Japan)/ethanol mixture (weight ratio of 1 : 1 g/g) for 6 h and subsequently immersed in a solution of epoxy resin for 12 h to completely swap the ethanol in the sample for the epoxy resin solution. The epoxy-resin-solution-impregnated sample was embedded in a silicon mold; subsequently, the epoxy resin solution was poured into the mold and cured at 343 K for 5 d. The resin block embedding the gel

sample was subsequently thin-sectioned using an ultramicrotome (UC7, Leica Microsystems GmbH, Wetzlar, Germany), and sections of thickness 100 nm were collected on a copper mesh TEM grid with a microgrid mesh and observed by FE-TEM. The acceleration voltage of the electron gun used for observation was 200 kV.

SiO_2/PDMAAm ratio measurement

Thermogravimetric (TG) measurement of the inorganic/organic composite skeleton was performed to calculate the SiO_2/PDMAAm ratio. The inorganic/organic composite skeleton was obtained from the inorganic/organic NC ion gels *via* IL extraction using a sufficient amount of ethanol followed by drying in vacuum at an elevated temperature. The TG measurement was conducted using open Pt pans on a thermogravimetry-differential thermal analysis device (TG-DTA Thermo plus EVO II, Rigaku Co., Tokyo, Japan) from 373 to 1273 K at a heating rate of 10 K min^{-1} under pure air (TAIYO NIPPON SANSO CORPORATION, Tokyo, Japan) atmosphere. Before the measurement, the sample atmosphere was maintained at 373 K for 2 h to remove the absorbed water. The PDMAAm weight was obtained as the weight loss from 373 to 1273 K. The SiO_2 weight was obtained as the residual weight at 1273 K.

Results and discussion

Mechanical behavior of the inorganic/organic NC ion gels

Fig. 1 shows the cyclic loading–unloading curves of the inorganic/organic DN and NC ion gels. As shown in Fig. 1(a), the inorganic/organic DN ion gel showed a clear mechanical hysteresis in the cyclic loading–unloading. The mechanical hysteresis observed in the inorganic/organic DN ion gel was resulted from the energy dissipation *via* the internal fracture of the silica particle network.[28] However, in the case of the inorganic/organic NC ion gel, as shown in Fig. 1(b), the stress–strain curve did not show a clear mechanical hysteresis. In other words, the mechanical property of the NC ion gel was almost elastic. It was reported that SR hydrogels did not indicate any mechanical hysteresis.[27] Therefore, this almost elastic mechanical property of the NC ion gel was consistent with that of SR hydrogel. The very small mechanical hysteresis observed in the cyclic loading–unloading curves in the NC ion gel would be attributed to the fracture of aggregated silica nanoparticles because silica particles were generally aggregated in the IL medium by interparticle attraction forces such as hydrogen bonding and van der Waals interaction.[29–33] However, comparing the stress–strain curves of the DN and NC ion gels, the hysteresis of the NC ion gel was much smaller than that of DN ion gel. Therefore, it can be considered that the extent of the silica nanoparticle aggregates ruptured in the NC ion gels would be much smaller than that in the DN ion gels.

On the other hand, we evaluated the relationship between toughness and dissipated energy of three kinds of inorganic/organic ion gels, *i.e.* NC, DN, and μ-DN ion gels. Here, μ-DN ion gel is a special type of DN ion gel with partially developed silica particle network.[34] The relationship between the dissipated energy and toughness of the NC, DN, and μ-DN ion gels with the same inorganic network composition is shown in Fig. 2. In this figure, it is clearly shown that the relationship between the dissipated energy and toughness of the DN and μ-DN ion gels showed the same trend. On the other hand, the NC ion gels showed a different tendency, *i.e.* the toughness was much higher than that of DN and μ-DN ion gels. Thus, it could be considered that the toughening mechanism of the NC ion gel would be completely different from the DN and μ-DN ion gels.

Effect of silica particle content on the mechanical properties of inorganic/organic NC ion gels

In the SR hydrogels, the stress–strain behavior is affected by the cross-linking density of the polyrotaxane network. For example, the fracture stress of the SR gels increased with increasing cross-linking density while the fracture strain was almost constant.[27] Therefore, if the toughening mechanism of the NC ion gel is the same as that of the SR gels, the fracture stress of the NC ion gels would be increased by increasing the cross-linking density of the silica particle-based aggregates. The cross-linking density could be controlled by the silica particle content. Thus, to evaluate the effect of cross-linking density of the silica particle-based aggregates on the mechanical properties of the NC ion gels, we prepared the NC ion gels with various

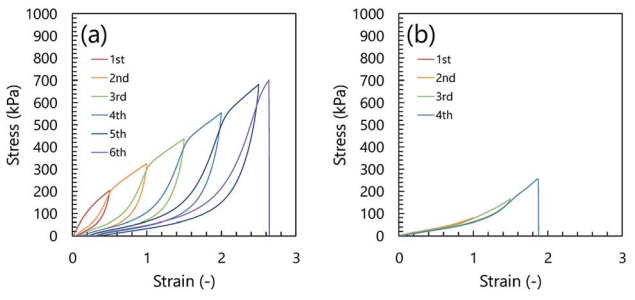

Fig. 1 Cyclic loading–unloading curves of inorganic/organic DN ion gel (a) and inorganic/organic NC ion gel (b). The SiO_2/PDMAAm weight ratio of the inorganic/organic DN and NC ion gels were 0.20 and 0.22, respectively.

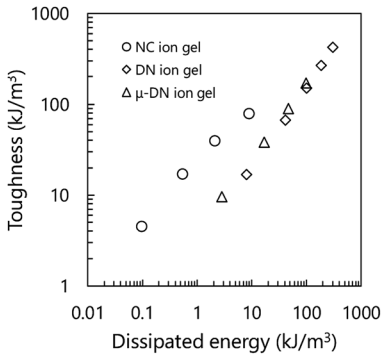

Fig. 2 Relationship between toughness and dissipated energy of inorganic/organic NC, DN, and μ-DN ion gels. The NC, DN, and μ-DN ion gels are prepared from the same precursor solution with 0.17 of TEOS/DMAAm molar ratio.

silica particle contents with an almost constant PDMAAm content. The experimentally determined composition of the prepared inorganic/organic NC ion gels are summarized in Table 1.

Fig. 3 shows the stress–strain curves of the inorganic/organic NC ion gels with various SiO_2/PDMAAm weight ratios. In Fig. 3, the line (a) (SiO_2/PDMAAm = 0) corresponds to the result of PDMAAm SN ion gel. It can be clearly found that the shapes of the stress–strain curves of the inorganic/organic NC ion gels were different from that of the PDMAAm SN ion gel. For the PDMAAm SN ion gel, the stress–strain curve showed no significant stress increase at high strain region. Meanwhile, the stress–strain curves of the inorganic/organic NC ion gels showed a significant stress increment at the high strain region, which was similar to the specific mechanical behavior of SR gels.[27] In addition, the inorganic/organic NC ion gels indicated a higher fracture stress than the PDMAAm SN ion gel. From these results, it was confirmed that the mechanical property of the inorganic/organic NC ion gels were significantly affected by the silica particle content. The effect of silica particle content on the fracture stress and fracture strain of the inorganic/organic NC ion gels are shown in Fig. 4(A) and (B), respectively. As shown in Fig. 4(A) and (B), the fracture stress of the inorganic/organic NC ion gels increased with the increase of the SiO_2/PDMAAm weight ratio although the fracture strain was almost constant in the range of 1.5–1.9. The properties shown in Fig. 3, 4(A) and (B) were consistent with those of SR gels.[27]

Furthermore, we evaluated the strain at the hardening point. We plotted stress σ against $\lambda - \lambda^{-2}$, where λ is strain +1. As shown in Fig. 4(C), the PDMAAm SN ion gel showed linear relationship between σ and $\lambda - \lambda^{-2}$. This indicated that the SN ion gel was neo-Hookean solid. On the other hand, the inorganic/organic NC ion gels showed non-linear relationship. The relationship deviated from $\sigma = G(\lambda - \lambda^{-2})$, where G is elastic modulus. This indicated the strain hardening occurred in the NC ion gels. We defined that the strain at the hardening point is that at which the difference between the applied σ and the calculated σ from $G(\lambda - \lambda^{-2})$ was 1 kPa. The strains at the hardening points determined from the above analysis were shown in Fig. 4(D). Additionally, to increase the reliability of the hardening point, we determined the strain at the hardening point as the strain at the local minimum of the differential stress–strain curve ($d\sigma/d\varepsilon$), where ε is strain. The relationship between $d\sigma/d\varepsilon$ and strain was shown in Fig. S1.† The determined strains at the hardening points were plotted in Fig. 4(D). As shown in Fig. 4(D), the determined strain at the hardening point monotonically decreased with increasing silica particle content.

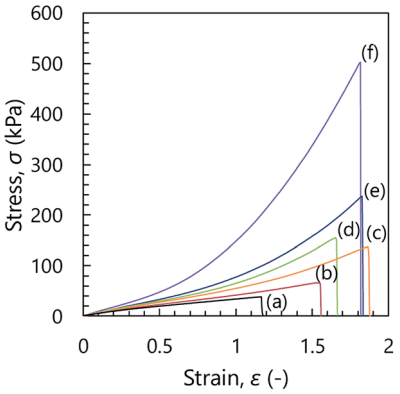

Fig. 3 Stress–strain curves of the inorganic/organic NC ion gels. SiO_2/PDMAAm (weight ratio) = 0 (a), 0.07 (b), 0.11 (c), 0.16 (d), 0.22 (e), and 0.32 (f). Line (a) corresponds to PDMAAm SN ion gel.

At the hardening point, the load applied to the gel network suddenly increases. This would mean that a large parts of gel networks became elongated state to sustain the applied load. If the gel network was randomly developed and had no special structure, the number of the gel network sustaining the applied force should gradually increase, as shown in the result of SN ion gel (Fig. 3(a)). In other words, the sudden increase of the applied stress to the gel suggested that the NC ion gel would have characteristic network structure, which was different from the SN and DN ion gels. In addition, it was considered that the ratio of the characteristic structure in whole of the developed network would be increased by the increase of the silica nanoparticles in the NC ion gel.

In order to confirm the silica nanoparticle originated characteristic network structure in the NC ion gel, we then observed the structure of the silica nanoparticles formed in the NC ion gels using TEM.

Table 1 Compositions of inorganic/organic NC ion gels prepared from precursor solutions with various TEOS/DMAAm molar ratios. The IL contents are obtained *via* IL extraction using sufficient ethanol followed by drying in a vacuum at an elevated temperature. The SiO_2 and PDMAAm contents in the inorganic/organic skeleton were calculated from the weight ratio of a silica particle and PDMAAm, which were obtained by TG measurement

TEOS/DMAAm molar ratio	IL content (wt%)	Silica particle content (wt%)	PDMAAm content (wt%)	SiO_2/PDMAAm weight ratio
0.5	77.3	5.5	17.2	0.32
0.33	79.4	3.6	17.0	0.22
0.25	81.1	2.6	16.3	0.16
0.20	82.1	1.9	15.9	0.12
0.17	82.3	1.8	16.0	0.11
0.10	82.4	1.1	15.5	0.07

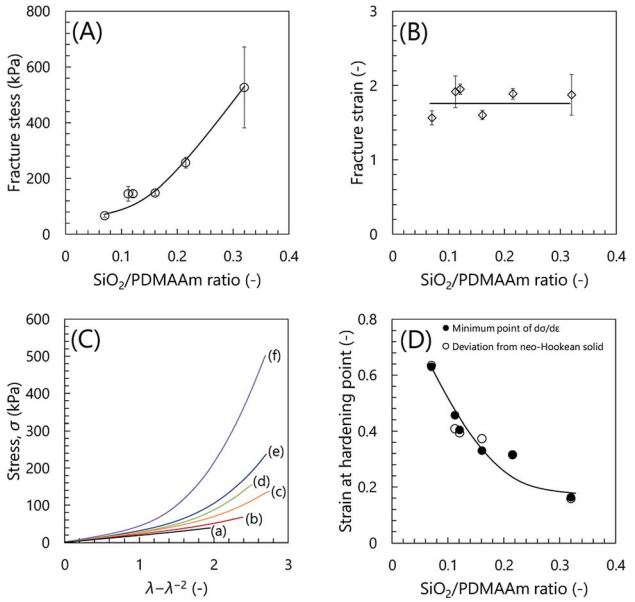

Fig. 4 (A), (B) Fracture stress and fracture strain as a function of SiO_2/PDMAAm weight ratio, respectively. (C) Relationship between σ and $\lambda - \lambda^{-2}$ of the inorganic/organic NC ion gels. SiO_2/PDMAAm (weight ratio) = 0 (a), 0.07 (b), 0.11 (c), 0.16 (d), 0.22 (e), and 0.32 (f). Line (a) corresponds to PDMAAm SN ion gel. (D) Strain at hardening point as a function of SiO_2/PDMAAm weight ratio.

Network structure of inorganic/organic NC ion gels

The structure of silica nanoparticles in the inorganic/organic NC ion gels was observed by TEM. The TEM images of the inorganic/organic NC ion gel are shown in Fig. 5. The dark part in the TEM images indicates the inorganic silica particles. As shown in Fig. 5(a) and (b), the silica particles formed very small aggregates, which were secondary silica nanoparticles, and the secondary silica nanoparticles were well dispersed in the inorganic/organic NC ion gel. The structure of the well-dispersed secondary silica nanoparticles in the inorganic/organic NC ion gel completely differed with the case of the inorganic/organic DN ion gel, which was composed of network-like silica nanoparticle aggregates with approximately several hundred nanometers shown in Fig. S2.†[34] Owing to the difference in size of the silica particle aggregates, the inorganic/organic NC ion gel was transparent although the inorganic/organic DN ion gel was translucent (Fig. S3†). In addition, because of the very small size of the secondary silica particles formed in the NC ion gel, it could be considered that the number of the secondary silica particles interpenetrating the polymer network was small. Therefore, the ruptured secondary silica particles during stretching test would be very small. As the result, as shown in Fig. 1, energy dissipated by the rupture of the secondary silica nanoparticles would be much smaller than that of the DN ion gel.

Subsequently, we discuss the detailed structure of the silica particles in the inorganic/organic NC ion gel. As shown in Fig. 5(c)–(f), secondary silica particles with approximately 12 nm diameter were composed of primary silica nanoparticles with approximately 3 nm diameter as indicated in Fig. 4(c) with white arrows. In addition, a low electron density region, which is shown as a lighter part than the primary silica particle in the TEM image shown in Fig. 5(c)–(f), appeared around the center of the secondary silica particles. It could be assumed that the low electron density region contained not only amorphous SiO_2, but also low electron density materials such as organic polymers. That is, the PDMAAm chain would be bored through the secondary silica particle. As the result, it was confirmed that a characteristic gel network composed of ring-like silica nanoparticle aggregates and PDMAAm chains were formed in the NC ion gel.

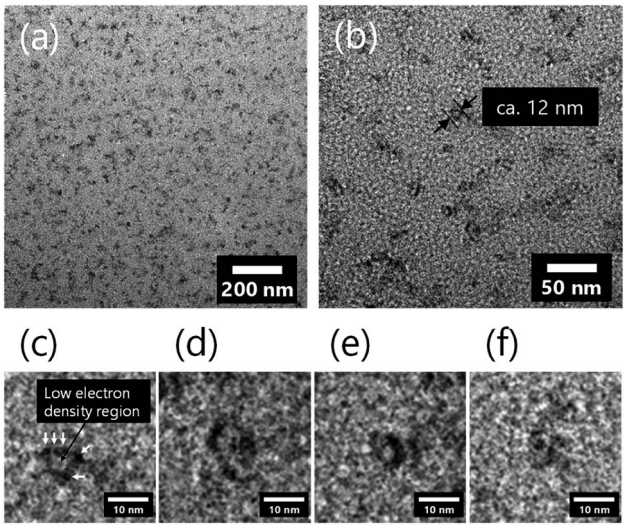

Fig. 5 Electron microscopy images of silica nanoparticles in inorganic/organic NC ion gel with SiO_2/PDMAAm weight ratio = 0.32. (a) Over view, (b) magnified view, and (c–f) ring-like silica nanoparticle aggregates. The white arrows in the (c) mean primary particles with *ca.* 3 nm diameter.

Possible toughening mechanism of the inorganic/organic NC ion gels

Considering the experimental results and comparing the mechanical properties of the NC ion gel and SR hydrogel, we considered several possibilities on the role of the silica nanoparticles on the increase of the mechanical strength of the NC ion gel.

Recently, Watanabe *et al.* reported that the inorganic/organic ion gel prepared using surface modified silica particles having negligibly low interaction between the silica nanoparticles had very low mechanical strength.[35] From this report, it is considered that the well-dispersed silica nanoparticles themselves could not increase the strength of the NC ion gel if the silica nanoparticles did not interact with polymer network. In other words, it could be said that the silica nanoparticles should have some interaction with each other or with PDMAAm to toughen the NC ion gel.

On the other hand, if the silica nanoparticles had strong interaction with the polymer network, the adsorption of PDMAAm to silica particles will be occurred. Such adsorption

was confirmed in silica particle/PDMAAm composite hydrogel system.[36] If the adsorption of PDMAAm on the silica nanoparticles occurred in our developed NC ion gels, the ion gels should show not only high mechanical strength but also large mechanical hysteresis in the cyclic stress loading–unloading test. However, the NC ion gels did not show large hysteresis. In addition, in our previous study, we demonstrated that PDMAAm hardly adsorbed on the silica particles in the ionic liquid medium.[28] Therefore, the adsorption of PDMAAm on silica particle cannot be the toughening mechanism of the inorganic/organic NC ion gel.

In addition, as shown in the TEM images of the NC ion gels (Fig. 5(a) and (b)), the silica nanoparticles formed no network-like structure in the NC ion gels. Therefore, the energy dissipation mechanism seen in the DN ion gel system was not the toughening mechanism of the NC ion gel.

Here, considering the experimental results in this work, from the TEM observation, it was suggested that the PDMAAm network and silica nanoparticles formed a characteristic ring-like structure of which PDMAAm bored through the very small silica nanoparticle-based aggregates consisted of a few silica nanoparticles. If silica nanoparticles formed such ring-like structure in the NC ion gel, it can be considered that the characteristic network could increase the mechanical strength of the NC ion gel according to the following two possible mechanisms. The first conceivable mechanism is the energy dissipation *via* the internal fracture of the small silica particle aggregates. However, in the cyclic stress loading–unloading test, the NC ion gel did not show large mechanical hysteresis (Fig. 1(b)). Thus, it is hard to consider that the energy dissipation along with the internal rupture of the silica nanoparticle aggregates was the main mechanism to toughen the NC ion gel. The other conceivable mechanism was the energy dispersion mechanism owing to the silica nanoparticle aggregates-based movable cross-linker. As mentioned before, the characteristic mechanical properties of the NC ion gels, such as the drastic stress increase at the high strain state (Fig. 3) and very low mechanical hysteresis (Fig. 1(b)), were also very similar to the mechanical property of SR gels. Therefore, because of the estimated network structure and the characteristic mechanical properties, we consider that the energy dispersion owing to the silica nanoparticle aggregate-based movable cross-linker would be the toughening mechanism of the NC ion gels.

The expected formation mechanism of the secondary silica particles incorporating PDMAAm chains in the inorganic/organic NC ion gel is shown in Fig. 6. The silica particle in inorganic/organic NC ion gel grew within the highly developed PDMAAm network. Therefore, it was reasonable to consider that the nuclear growth of the silica particle started on the PDMAAm chain and subsequently, secondary silica particles grew around the PDMAAm chains. This implies that PDMAAm chains were incorporated in a secondary silica particle *via* the nuclear growth of the silica particle. As the result, the low electron density region in the secondary silica particles were observed in the TEM images of the NC ion gels. According to this hypothesis, it could be considered that the secondary silica particles incorporating a PDMAAm chain acted as a movable cross-linker for the PDMAAm network in the inorganic/organic NC ion gels.

Based on these results, the schematics of the estimated network structure of the inorganic/organic NC ion gel are as shown in Fig. S4.† The gel network of the inorganic/organic NC ion gel was composed of secondary silica particles and a PDMAAm network. The secondary silica particles dispersed well in the gel and incorporated PDMAAm chains *via* particle growth. The secondary silica particles incorporating more than two PDMAAm chains served as a movable cross-linker in the gel, while the secondary silica particle incorporating only one PDMAAm chain was not a cross-linker.

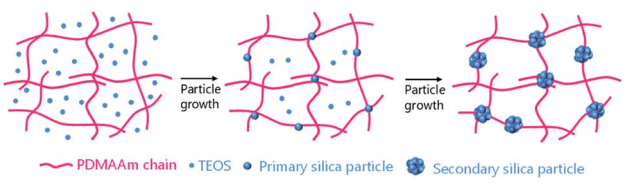

Fig. 6 Schematics of formation mechanism of secondary silica particle incorporating PDMAAm chains in the inorganic/organic NC ion gels.

Conclusion

In this study, the reasonable network structure and toughening mechanism of the inorganic/organic NC ion gel were estimated. Structural observation results indicated that the secondary silica particles were well dispersed in the inorganic/organic NC ion gel. In addition, the secondary silica particles would incorporate PDMAAm chains. Based on the network formation process, the silica particle grew in the highly developed PDMAAm network. In this case, the nuclear growth of silica particle would start on the PDMAAm chain. Therefore, it could be considered that the secondary silica particles formed ring-like structure, incorporated PDMAAm chains, and acted as a movable cross-linker of the PDMAAm chains. Because of the sliding motion by secondary silica particles, the inorganic/organic NC ion gels could exhibit characteristic stress increase when it was highly elongated.

Conflicts of interest

There are no conflicts to declare.

Acknowledgements

The authors thank the Research Facility Center for Science and Technology of Kobe University for providing FE-TEM for this study. Parts of this work were supported by KAKENHI (18K04812 and 19J11528) of the Japan Society for the Promotion of Science (JSPS).

References

1 A. Noda and M. Watanabe, *Electrochim. Acta*, 2000, **45**, 1265–1270.

2 J. Ding, D. Zhou, G. Spinks, G. Wallace, S. Forsyth, M. Forsyth and D. MacFarlane, *Chem. Mater.*, 2003, **15**, 2392–2398.
3 T. Ueki and M. Watanabe, *Macromolecules*, 2008, **41**, 3739–3749.
4 J. E. Bara, E. S. Hatakeyama, D. L. Gin and R. D. Noble, *Polym. Adv. Technol.*, 2008, **19**, 1415–1420.
5 T. P. Lodge, *Science*, 2008, **321**, 50–51.
6 M. Armand, F. Endres, D. R. MacFarlane, H. Ohno and B. Scrosati, *Nat. Mater.*, 2009, **8**, 621–629.
7 J. Lu, F. Yan and J. Texter, *Prog. Polym. Sci.*, 2009, **34**, 431–448.
8 J. Le Bideau, J. B. Ducros, P. Soudan and D. Guyomard, *Adv. Funct. Mater.*, 2011, **21**, 4073–4078.
9 D. L. Gin and R. D. Noble, *Science*, 2011, **332**, 674–676.
10 S. Imaizumi, H. Kokubo and M. Watanabe, *Macromolecules*, 2012, **45**, 401–409.
11 S. Kasahara, E. Kamio, R. Minami and H. Matsuyama, *J. Membr. Sci.*, 2013, **431**, 121–130.
12 S. Kasahara, E. Kamio, A. Yoshizumi and H. Matsuyama, *Chem. Commun.*, 2014, **50**, 2996–2999.
13 F. Moghadam, E. Kamio, A. Yoshizumi and H. Matsuyama, *Chem. Commun.*, 2015, **51**, 13658–13661.
14 F. Ranjbaran, E. Kamio and H. Matsuyama, *J. Membr. Sci.*, 2017, **544**, 252–260.
15 K. Fujii, A. Hanako, T. Ueki, T. Sakai, S. Imaizumi, U. Chung, M. Watanabe and M. Shibayama, *Soft Matter*, 2012, **8**, 1756–1759.
16 Y. Gu, S. Zhang, L. Martinetti, K. H. Lee, L. D. McIntosh, C. D. Frisbie and T. P. Lodge, *J. Am. Chem. Soc.*, 2013, **135**, 9652–9655.
17 H. Arafune, S. Honma, T. Morinaga, T. Kamijo, M. Miura, H. Furukawa and T. Sato, *Adv. Mater. Interfaces*, 2017, **4**, 1700074.
18 Y. Ding, J. Zhang, L. Chang, X. Zhang, H. Liu and L. Jiang, *Adv. Mater.*, 2017, **29**, 1704253.
19 F. Moghadam, E. Kamio and H. Matsuyama, *J. Membr. Sci.*, 2017, **525**, 290–297.
20 F. Moghadam, E. Kamio, T. Yoshioka and H. Matsuyama, *J. Membr. Sci.*, 2017, **530**, 166–175.
21 E. Kamio, T. Yasui, Y. Iida, J. P. Gong and H. Matsuyama, *Adv. Mater.*, 2017, **29**, 1704118.
22 Y. Okumura and K. Ito, *Adv. Mater.*, 2001, **13**, 485–487.
23 K. Ohmori, I. Abu Bin, T. Seki, C. Liu, K. Mayumi, K. Ito and Y. Takeoka, *Chem. Commun.*, 2016, **52**, 13757–13759.
24 K. Kato, Y. Okabe, Y. Okazumi and K. Ito, *Chem. Commun.*, 2015, **51**, 16180–16183.
25 A. B. Imran, K. Esaki, H. Gotoh, T. Seki, K. Ito, Y. Sakai and Y. Takeoka, *Nat. Commun.*, 2014, **5**, 5124.
26 K. Kato, Y. Ikeda and K. Ito, *ACS Macro Lett.*, 2019, **8**, 700–704.
27 K. Ito, *Polym. J.*, 2007, **39**, 489–499.
28 T. Yasui, S. Fujinami, T. Hoshino, E. Kamio and H. Matsuyama, *Soft Matter*, 2020, **16**, 2363–2370.
29 K. Ueno, K. Hata, T. Katakabe, M. Kondoh and M. Watanabe, *J. Phys. Chem. B*, 2008, **112**, 9013–9019.
30 K. Ueno, A. Inaba, M. Kondoh and M. Watanabe, *Langmuir*, 2008, **24**, 5253–5259.
31 J. Nordström, L. Aguilera and A. Matic, *Langmuir*, 2012, **28**, 4080–4085.
32 K. Ueno, S. Imaizumi, K. Hata and M. Watanabe, *Langmuir*, 2009, **25**, 825–831.
33 H. C. Chang, T. C. Hung, S. C. Chang, J. C. Jiang and S. H. Lin, *J. Phys. Chem. C*, 2011, **115**, 11962–11967.
34 T. Yasui, E. Kamio and H. Matsuyama, *Langmuir*, 2018, **34**, 10622–10633.
35 T. Watanabe, R. Takahashi and T. Ono, *Soft Matter*, 2020, **16**, 1572–1581.
36 W. C. Lin, W. Fan, A. Marcellan, D. Hourdet and C. Creton, *Macromolecules*, 2010, **43**, 2554–2563.